Facile Formation of Redox-Active Totally Organic Nanoparticles in Water by In Situ Reduction of Organic Precursors Stabilized through Aromatic–Aromatic Interactions by Aromatic Polyelectrolytes

Mario E. Flores, Pablo Garcés-Jerez, Daniel Fernández, Gustavo Aros-Perez, Diego González-Cabrera, Eduardo Álvarez, Ignacio Cañas, Felipe Oyarzun-Ampuero, Ignacio Moreno-Villoslada*

The formation of redox-active, totally organic nanoparticles in water is achieved following a strategy similar to that used to form metal nanoparticles. It is based on two fundamental concepts: i) complexation through aromatic–aromatic interactions of a water-soluble precursor aromatic molecule with polyelectrolytes bearing complementary charged aromatic rings, and ii) reduction of the precursor molecule to achieve stabilized nanoparticles. Thus, formazan nanoparticles are synthesized by reduction of a tetrazolium salt with ascorbic acid using polyelectrolytes bearing benzene sulfonate residues of high linear aromatic density, but cannot be formed in the presence of nonaromatic polyelectrolytes. The red colored nanoparticles are efficiently encapsulated in calcium alginate beads, showing macroscopic homogeneity. Bleaching kinetics with chlorine show linear rates on the order of tenths of millimeters per minute. A linear behavior of the dependence of the rate of bleaching on the chlorine concentration is found, showing the potential of the nanoparticles for chlorine sensing.

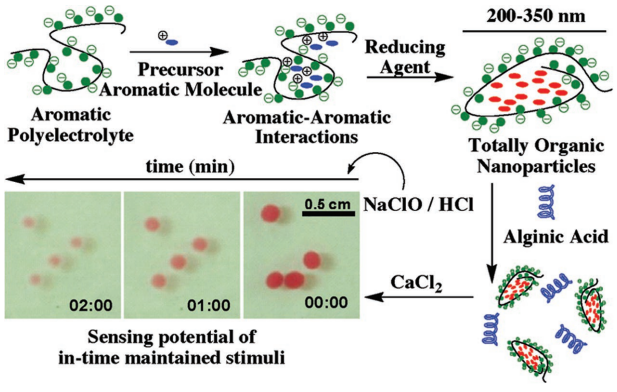

Dr. M. E. Flores, P. Garcés-Jerez, D. Fernández, G. Aros-Perez, D. González-Cabrera, E. Álvarez, I. Cañas, Prof. I. Moreno-Villoslada
Instituto de Ciencias Químicas
Facultad de Ciencias
Universidad Austral de Chile
Las Encinas 220, Valdivia 5110033, Chile
E-mail: imorenovilloslada@uach.cl
Dr. F. Oyarzun-Ampuero
Departamento de Ciencias y Tecnología Farmaceútica
Facultad de Ciencias Químicas y Farmacéuticas
Universidad de Chile
Santos Dumont 964, Santiago 8380494, Chile

1. Introduction

The synthesis of metal nanoparticles, such as gold, silver, or copper nanoparticles relies mainly on a reduction reaction of metal ions in the presence of additives used to initiate and control the reaction.[1] On the other hand, the synthesis of organic and bioorganic nanoparticles can be achieved using different approaches. Complementary charged molecules and macromolecules may form nanoprecipitates by ionic self-assembly.[2–4] Hydrophobic molecules may form nanosolids through emulsification of the target molecule dissolved in an organic solvent and

DOI: 10.1002/marc.201600339

further evaporation of the solvent.[5] An alternative one-step procedure consists of nanoprecipitation through solvent displacement, for which, the hydrophobic molecule must be soluble in a water-soluble organic solvent.[6] It is clear from the above statements that fundamentally different strategies are used to produce metal nanoparticles and organic nanoparticles, the former based on a redox reaction as the main step of synthesis, and the latter based on the physics of molecular assembly and phase separation. As far as we know, no literature can be found for totally organic nanoparticle formation through an organic solvent-free procedure based on in situ redox reactions in the presence of stabilizers, thus applying the strategy used for inorganic nanoparticles.

In the last few years, we have shown that polyelectrolytes bearing charged aromatic groups interact with aromatic counterions not only by long-range electrostatic interactions, but also through short-range aromatic–aromatic interactions, which lead to site-specific binding.[7–15] Aromatic–aromatic interactions are attracting much attention nowadays, since they explain the structure stabilization of many supramolecular assemblies, molecular recognition in enzymatic activity, stabilization of the tertiary structure of proteins, and stacking of DNA base pairs.[16,17] These interactions provide higher binding constants between the two interacting species, and resistance to the cleaving effect of the presence of electrolytes such as NaCl. In addition, they have shown potential for tuning molecular properties of the counterions, such as luminescent,[18] redox,[19] and acid-base[8] properties. Systems undergoing aromatic–aromatic interactions have been investigated for drug delivery and chemical catalysis.[20,21] Studied aromatic polymers include those bearing benzene sulfonate (BS) residues, such as poly(sodium 4-styrenesulfonate) (PSS) and its copolymers with maleate, poly(sodium 4-styrenesulfonate-*co*-sodium maleate) at comonomer compositions of 3:1 and 1:1 [P(SS_3-*co*-MA_1) and P(SS_1-*co*-MA_1)], showing different linear aromatic density.[22–24] The structure of these polymers are shown in Figure SI1 of the Supporting Information.

Among aromatic counterions, the tetrazolium salt 2,3,5-triphenyl-2*H*-tetrazolium chloride (TTC) has been used.[9–11] It was seen by diafiltration and ^{1}H-NMR, that aromatic–aromatic interactions between the tetrazolium salt and polymers bearing BS groups occur, and the strength of the interaction directly correlates with the linear aromatic density. TTC is commonly used as an indicator due to its staining properties, since it can be reduced to the corresponding red formazan, 1,3,5-triphenylformazan (TF), and has been used in various biological applications, such as counting bacterial colonies or testing viability of seeds, measuring mitochondrial activity.[21] On the other hand, the red TF can be oxidized with an oxidizing agent causing its discoloration.

As a redox-active pair of molecules, the system TTC/TF represents a good couple for the synthesis of organic nanoparticles of TF by reduction of the precursor TTC, through a strategy similar to that used for the synthesis of metal nanoparticles. These nanoparticles may be useful for sensing purposes, since the oxidation of TF involves color change. In this communication, we will demonstrate that such TF nanoparticles may be produced in water, thus, without using any organic solvent, in the presence of anionic polyelectrolytes showing high linear density of BS groups as stabilizers, but not in the presence of nonaromatic polyelectrolytes, highlighting the role of aromatic–aromatic interactions in the system stabilization. In addition, we will show that the nanoparticles can be homogeneously dispersed in calcium alginate beads (CAB), showing potential as handleable chlorine colorimetric sensors.

2. Results and Discussion

The reduction of TTC to TF in water has been achieved in the presence of ascorbic acid (ASC) in basic media, following Scheme 1, and as detailed in the Supporting Information. As can be seen in Figure 1, reduction of 1×10^{-3} M of TTC with 2×10^{-3} M of ASC in the presence of 1.6×10^{-1} M of NaOH, produces precipitates of the red TF. The same result is obtained in the presence of 1×10^{-2} M of the nonaromatic polyelectrolyte poly(sodium acrylate-*co*-sodium maleate) at a comonomer composition 1:1 [P(AA_1-*co*-MA_1], and even in the presence of P(SS_1-*co*-MA_1), which presents the lowest linear BS density. On the contrary, those with higher linear aromatic density, namely, P(SS_3-*co*-MA_1) and PSS, produced red, turbid suspensions. The concentration of the aromatic polymers was also set at 1×10^{-2} M given in mol

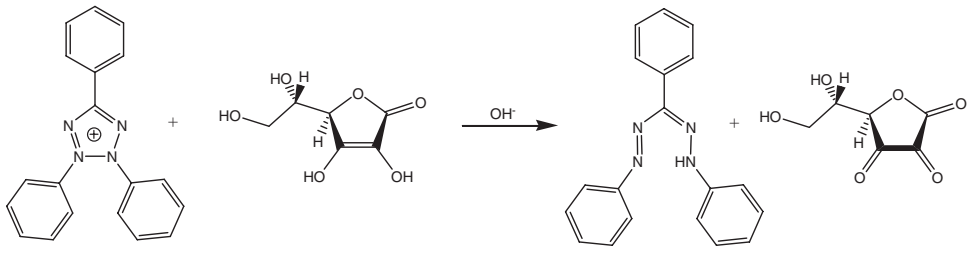

Scheme 1. TTC reduction by ascorbic acid.

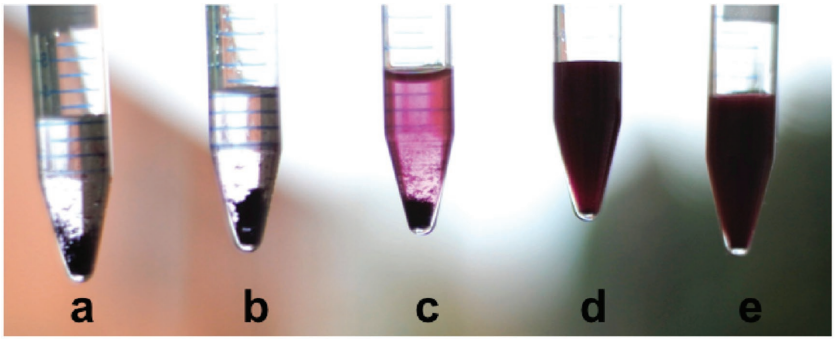

Figure 1. Samples after reduction of 1×10^{-3} M of TTC a) in the absence of any polyelectrolyte and b) in the presence of 1×10^{-2} M of P(AA_1-*co*-MA_1), c) P(SS_1-*co*-MA_1), d) P(SS_3-*co*-MA_1), and e) PSS.

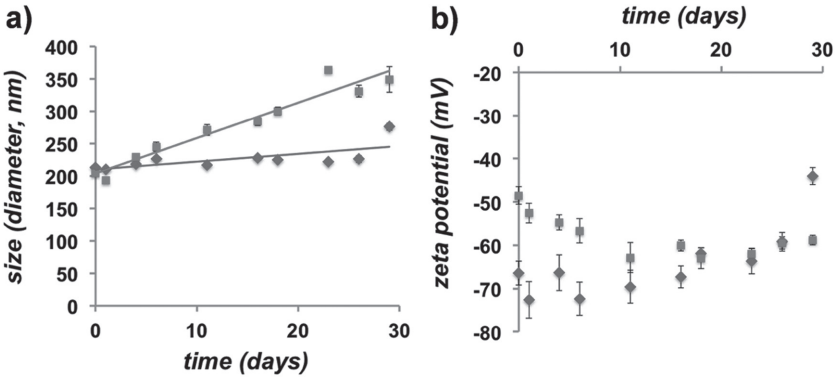

Figure 2. a) Hydrodynamic diameter and b) zeta potential of TF/PSS (◆) and TF/P(SS_3-*co*-MA_1) (■) nanoparticles suspended in water during 30 d (with SD, $n = 3$) at 25 °C.

of BS groups per liter, so that, all samples present the same number of BS groups and increasing number of polymeric negative charges as the linear aromatic density decreases.

The colloids formed in the presence of PSS and P(SS_3-*co*-MA_1) have nanometric apparent size, ranging between 200 and 350 nm, showing polydispersity indexes lower than 0.2, and negative zeta potentials lower than –40 mV, as seen by dynamic light scattering experiments. The high absolute value of the zeta potential ensures stability of the colloidal suspensions, a fact that was corroborated by the analysis of size and zeta potential during 30 d. The results can be seen in Figure 2. In addition, the colloidal suspensions were subjected to 5 cycles of centrifugation at 15 000 rpm, resuspension in water, and sonication for 10 min, conserving after each cycle their size, low polydispersity index, and low zeta potential (data not shown), which confirm the high physical stability of the samples.

Nanosystems of PSS/TTC and P(SS_3-*co*-MA_1)/TTC have been reported,[10] which are rationally considered as aggregates produced through ion pair aggregation, the ion pairs occurring by complexation between the positively charged aromatic tetrazolium and the negatively charged aromatic BS groups, and stabilized by aromatic–aromatic interactions. Here, due to the low solubility of TF in water and its electroneutrality, the colloidal suspensions are rationally considered as nanoprecipitates of TF stabilized by the polyelectrolytes which should be found at the interface. STEM experiments confirm this, as can be seen in Figure 3, where particles with diameters close to those found by dynamic light scattering are observed for both TF/PSS and TF/P(SS_3-*co*-MA_1) systems.

Stopped-flow spectrometric measurements have been done during TTC reduction, and the reaction kinetics was

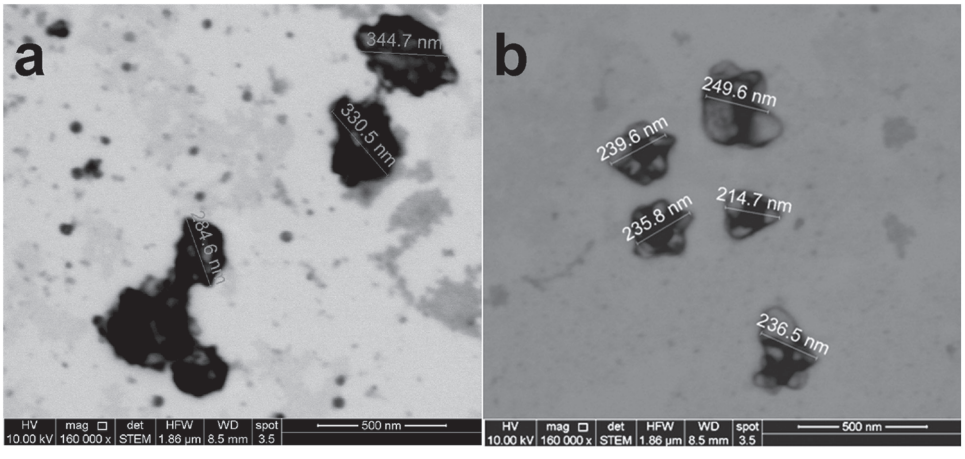

Figure 3. STEM images of a) TF/PSS and b) TF/P(SS_3-*co*-MA_1) nanoparticles.

Table 1. Activation Gibbs energy (E_a) for the reduction of TTC in the presence of ASC in the absence and in the presence of studied polyelectrolytes.

System	E_a [kJ mol^{-1}]
TF	80
TF/P(AA_1-*co*-MA_1)	114
TF/P(SS_1-*co*-MA_1)	109
TF/P(SS_3-*co*-MA_1)	114
TF/PSS	123

evaluated following the absorption at 524 nm during 80 s at different temperatures. The corresponding saturation curves (see Figure SI2, Supporting Information) showed a zero-order behavior in the first 20 s, and, applying a zero-order kinetics model, the kinetic constant dependent on the temperature $k(T)$ was obtained. The obtained $k(T)$ values follow the Arrhenius equation (see Figure SI3, Supporting Information), which allowed calculating the activation Gibbs energy (E_a) of the reaction. The results are presented in Table 1. The formation of TF/PSS nanoparticles presents the highest activation energy (123 kJ mol^{-1}), which may be related with a higher stabilization of TTC by aromatic–aromatic interactions.

The nanoparticles formed with PSS and P(SS_3-*co*-MA_1) were incorporated in CAB, thus generating a handleable material. CAB were formed by mixing a 3% alginate aqueous solution and the formed TF/PSS and TF/P(SS_3-*co*-MA_1) nanoparticle suspensions in a volume proportion of 1:1, and further dripping on a 0.1 M calcium chloride solution in water. The resulting beads showed the complexes homogenously dispersed, conserving the red color of the formazan (see Figure 4). The inclusion of TF, TF/P(AA_1-*co*-MA_1), and TF/P(SS_1-*co*-MA_1) did not produce a homogeneous distribution of the complexes into the CAB. Another strategy to include TF in CAB consisted on the previous encapsulation of TTC, complexed or not with any polyelectrolyte, and further reduction with ASC. However, this strategy resulted unsuccessful due to that under the strong alkaline conditions needed for reduction, calcium hydroxide is formed as a precipitate. Moreover, the retention of the readily water-soluble TTC in the CAB is low due to that the high ionic strength of the reaction medium produces cleaving of the TTC/polymer interaction, and consequently a fast diffusion of the tetrazolium salt into the bulk. Thus, the formation of TF nanoparticles, stabilized by PSS and P(SS_3-*co*-MA_1) previous to its encapsulation is revealed as an effective method to achieve handleable beads, macroscopically homogenous, which avoid the release of TF to the bulk, and the use of organic solvents.

TF can be oxidized by various oxidizing agents such as chlorine. By mixing aqueous solutions of sodium hypochlorite and hydrochloric acid at a 1:2 ratio to produce chlorine, instantaneous discoloration of noncomplexed TF occurred. We explored the behavior of the CAB containing TF/PSS and TF/P(SS_3-*co*-MA_1) nanoparticles in the presence of chlorine when an excess of the oxidizing agent over the TF amount ranging between 20 and 100-fold is maintained in time. It can be seen in Figure 4 that the CAB undergo discoloration in the lapse of 3 min at a NaOCl concentration of 0.02 M. The discoloration occurs from the outer surface toward the center of the CAB. Image analysis of the bleaching reaction allows obtaining the rough contour of the nondiscolored region projection in the x/y plane. Results revealed that the radius of the remaining colored spheres decreases linearly with time, as can be seen in Figure 5. The slope of the corresponding linear adjustment to the data may be considered as the linear bleaching rate (β) measured in length versus time units. The β values found stood in the range of tenths of millimeters per minute, and are a function of the chlorine concentration.

The increase of the absolute value of β with the increase on the NaOCl concentration does also follow a linear function, as shown in Figure 5c, showing the potential of the materials for chlorine sensing when the stimuli is maintained in time. The slope of the linear tendency may have the physical meaning of a concentration resistance coefficient (γ, cm M^{-1} s^{-1}) of the CAB to be discolored. The corresponding γ values for the CAB containing TF/PSS and TF/P(SS_3-*co*-MA_1) nanoparticles are 0.025 and 0.026 cm M^{-1} s^{-1}, respectively, indicating that the resistance of TF bleaching is not related to the aromatic polymer used to stabilize the nanoprecipitates.

The results shown here open several research lines of scientific and technological relevance. Concerning the model molecules, this work highlights the potential of aromatic–aromatic interactions to direct chemical reactions. In the synthesis of metal nanoparticles, the

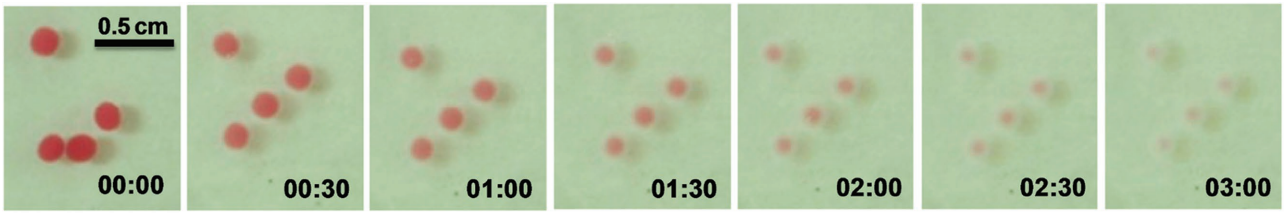

Figure 4. CAB with TF nanoparticles formed at t = 0, and its discoloration in a 0.02 M NaOCl/0.04 M HCl solution during 3 min.

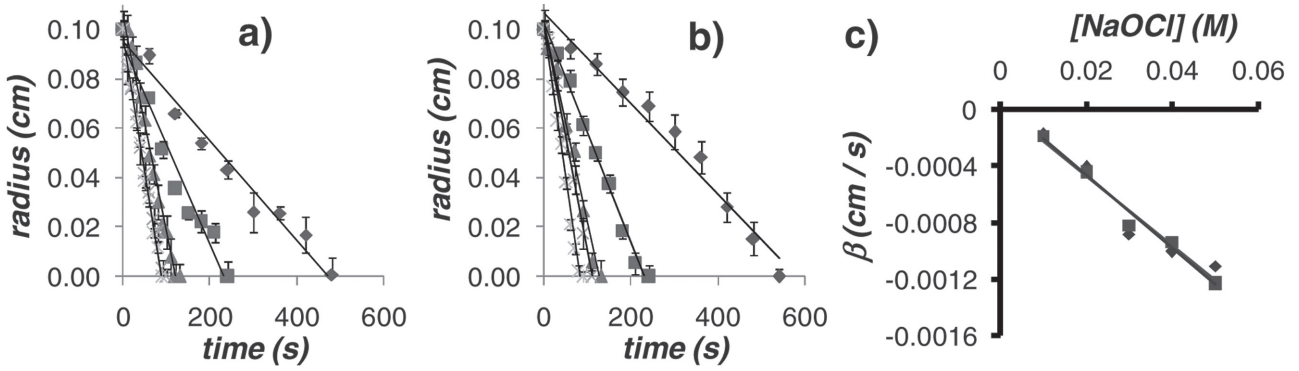

Figure 5. a,b) Radius of colored volume in CAB containing TF/PSS (a) and TF/P(SS_3-*co*-MA_1) (b) nanoparticles as a function of time in the presence of NaOCl in acidic media at concentrations of 1×10^{-2} (◆), 2×10^{-2} (■), 3×10^{-2} (▲), 4×10^{-2} (×), and 5×10^{-2} M (*), and c) corresponding β values as a function of NaOCl concentration.

ability of the stabilizer to chelate the precursor metal ions is pivotal. We demonstrate here that ionic interactions are not enough to allow the formation of TF nanoparticles, but short-range aromatic–aromatic interactions that promote the release of water from the hydration sphere of the precursor aromatic molecules are needed. Since aromatic–aromatic interactions between PSS or P(SS_3-*co*-MA_1) and TTC involve the close contact between the low molecular-weight molecule and the polymeric BS groups,[10] the reduction of TTC is achieved in the polymer domain or at the interface with bulk water, thus allowing the stabilization of the hydrophobic TF in the form of nanoparticles. In this sense, another striking projection of the discoverings made here is the study of the role of charged aromatic polyelectrolytes as molecular reactors to synthesize totally organic nanoparticles through other types of reactions involving aromatic reactants, such as electrophilic aromatic substitution. Molecular reactors are mainly based on molecules able to produce inclusion complexes, allowing changes on guest molecules reaction kinetics or obtaining products that would not be formed in the absence of the reactors. Polyelectrolytes such as PSS have been also used as molecular reactors and stabilizers in the synthesis of inorganic nanoparticles,[23–25] but, to the best of our knowledge, not to synthesize totally organic nanoparticles through redox reactions. The role of PSS and P(SS_3-*co*-MA_1) as molecular reactors to produce totally organic nanoparticles through reduction of precursor organic molecules is conceptually an absolute novelty of this work. In addition, we should account for the role of these polymers as stabilizers of hydrophobic totally organic nanoparticles. On the other hand, we also highlight the potential of stabilized polymer/TF nanoparticles as colorimetric responsive materials. Finally, we point at CAB as simple-to-handle devices that may be used as sensors, based on a dual role as carriers of colorimetric responsive materials, and materials able to tune response dynamics to in-time maintained stimuli by means of their swelling and permeability properties. Thus, formulated CAB can be used to sense process end-points, average flow-rates, or average concentration in time.[26,27] In addition, the biocompatibility of CAB promotes them as sensing materials in biological systems.[28]

Concerning the procedures, we highlight here a new strategy to form totally organic, redox-active nanoparticles that may also be projected for the synthesis of organic nanoparticles with other kind of activity. The formation of the aimed TF/polymer nanoparticles constitutes an absolute novelty of this work, not only because of the molecules used, but also because of the principles underlying the nanoprecipitation process, based on the complexation by aromatic–aromatic interactions of a water-soluble precursor molecule, in this case TTC, with a polyelectrolyte bearing complementary charged aromatic rings showing a high linear aromatic density, and further reduction of the precursor molecule to achieve stabilized nanoparticles, avoiding the use of any organic solvent. In addition, this work also furnishes a methodology to incorporate hydrophobic molecules into CAB also without using organic solvents, and preserving their stability during the formation process of the hydrogel.

3. Conclusions

TF/PSS and TF/P(SS_3-*co*-MA_1) nanoparticles have been synthesized in water by in situ reduction of the precursor TTC with ASC. The stabilized nanoparticles could be easily incorporated in CAB, and the potential of the resulting devices for colorimetric sensing of oxidants such as chlorine has been demonstrated. For the nanoparticles to be formed, the precursor molecule must be complexed with charged aromatic polyelectrolytes, subjected to aromatic–aromatic interactions. The results shown here highlight the potential of aromatic–aromatic

interactions to direct chemical reactions, and the role of charged aromatic polyelectrolytes as molecular reactors to produce totally organic nanoparticles involving aromatic molecules. The concepts involved in this research and the simplicity of the methods used confers a great value toward possible applications both in the research and in the industry fields.

Supporting Information

Supporting Information is available from the Wiley Online Library or from the author.

Acknowledgements: The authors thank Fondecyt Regular 1120514, 1150899, and 1161450.

Received: June 6, 2016; Revised: July 12, 2016; Published online: September 12, 2016; DOI: 10.1002/marc.201600339

Keywords: dyes, pigments; hydrogels; nanoparticles; pigments; polyelectrolytes; sensors

[1] Y. Sun, Y. Xia, *Science* **2002**, *298*, 2176.
[2] C. F. J. Faul, M. Antonietti, *Adv. Mater.* **2003**, *15*, 673.
[3] F. Gröhn, K. Klein, S. Brand, *Chem. Eur. J.* **2008**, *14*, 6866.
[4] C. F. J. Faul, *Acc. Chem. Res.* **2014**, *47*, 3428.
[5] R. L. McCall, R. W. Sirianni, *J. Vis. Exp.* **2013**, 51015.
[6] E. Piñón-Segundo, A. Ganem-Quintanar, J. R. Garibay-Bermúdez, J. J. Escobar-Chávez, M. López-Cervantes, D. Quintanar-Guerrero, *Pharm. Dev. Technol.* **2006**, *11*, 493.
[7] I. Moreno-Villoslada, M. Jofré, V. Miranda, P. Chandía, R. González, S. Hess, B. L. Rivas, C. Elvira, J. San Román, T. Shibue, H. Nishide, *Polymer* **2006**, *47*, 6496.
[8] I. Moreno-Villoslada, F. González, B. L. Rivas, T. Shibue, H. Nishide, *Polymer* **2007**, *48*, 799.
[9] I. Moreno-Villoslada, F. Gonzalez, L. Rivera, S. Hess, B. L. Rivas, T. Shibue, H. Nishide, *J. Phys. Chem. B* **2007**, *111*, 6146.
[10] I. Moreno-Villoslada, C. Torres, F. Gonzalez, M. Soto, H. Nishide, *J. Phys. Chem. B* **2008**, *112*, 11244.
[11] I. Moreno-Villoslada, M. Soto, F. Gonzalez, F. Montero-Silva, S. Hess, I. Takemura, K. Oyaizu, H. Nishide, *J. Phys. Chem. B* **2008**, *112*, 5350.
[12] I. Moreno-Villoslada, C. Torres, F. González, T. Shibue, H. Nishide, *Macromol. Chem. Phys.* **2009**, *210*, 1167.
[13] I. Moreno-Villoslada, C. Torres-Gallegos, R. Araya-Hermosilla, H. Nishide, *J. Phys. Chem. B* **2010**, *114*, 4151.
[14] C. Toncelli, J. P. Pino-Pinto, N. Sano, F. Picchioni, A. A. Broekhuis, H. Nishide, I. Moreno-Villoslada, *Dyes Pigm.* **2013**, *98*, 51.
[15] J. P. Fuenzalida, M. E. Flores, I. Móniz, M. Feijoo, F. Goycoolea, H. Nishide, I. Moreno-Villoslada, *J. Phys. Chem. B* **2014**, *118*, 9782.
[16] C. A. Hunter, J. K. M. Sanders, *J. Am. Chem. Soc.* **1990**, *112*, 5525.
[17] E. A. Meyer, R. K. Castellano, F. Diederich, *Angew. Chem. Int. Ed.* **2003**, *42*, 1210.
[18] I. Moreno-Villoslada, F. González, L. Arias, J. M. Villatoro, R. Ugarte, S. Hess, H. Nishide, *Dyes Pigm.* **2009**, *82*, 401.
[19] S. K. Sharma, R. Kumar, S. Kumar, R. Mosurkal, V. S. Parmar, L. A. Samuelson, A. C. Watterson, J. Kumar, *Chem. Commun.* **2004**, 2689.
[20] S. Fruhbeisser, F. Grohn, *J. Am. Chem. Soc.* **2012**, *134*, 14267.
[21] A. W. Nineham, *Chem. Rev.* **1955**, *55*, 355.
[22] C. J. Easton, S. F. Lincoln, L. Barr, H. Onagi, *Chem. Eur. J.* **2004**, *10*, 3120.
[23] J. H. Youk, J. Locklin, C. Xia, M.-K. Park, R. Advincula, *Langmuir* **2001**, *17*, 4681.
[24] D. G. Shchukin, G. B. Sukhorukov, *Adv. Mater.* **2004**, *16*, 671.
[25] J. Dai, M. L. Bruening, *Nano Lett.* **2002**, *2*, 497.
[26] S. Seo, J. Lee, M. S. Kwon, D. Seo, J. Kim, *ACS Appl. Mater. Interfaces* **2015**, *7*, 20342.
[27] C. Lee, S.-Y. Lee, *J. Ind. Eng. Chem.* **2016**, *38*, 67.
[28] J. Weidling, S. Sameni, J. R. T. Lakey, E. Botvinick, *J. Biomed. Opt.* **2014**, *19*, 087006.